

Analysis of coupled Vivaldi antenna elements for millimeter wave communication

Ismail Alaoui Abdallaoui, Laurent Leyssenne, Sidina Wane, Philippe Descamps, Hassan Kabbaj, Dominique Lesénéchal, Than Vinh Dinh

Abstract— In this paper, modeling and experimental characterization of coupled Vivaldi antenna elements printed on laminate substrate are proposed for Millimeter-Wave communication and Energy Harvesting. Both Time-Domain and Frequency domain electromagnetic simulations are conducted and compared to broadband measurement accounting for parasitic feeding effects (SMA connectors, wiring connections) also, evaluation of gain and radiation efficiencies. Perspectives for Co-integration of proposed Vivaldi antenna elements with power generation circuit blocks (VCO, Power Amplifier).

Index Terms— Vivaldi antenna; PCB Co-Design; Multi-Port measurement, Broadband deem-bedding; Numerical methods; UWB applications

1 INTRODUCTION

THE Ultra-Wide-Bandwidth (UWB) technology represents a very promising solution for the next generation applications, for overcoming current limitations with narrow bandwidth constraints. Expected main improvements include the following [1-3]:

- Reduced area coverage (Power Spectrum management).
- Insufficient ranging for accurate localization of mobile systems (e.g., RFID objects).
- Sensitivity to interference (e.g., adjacent channel multi-user couplings).
- Scarce multiple-access capabilities (e.g., MIMO architectures).

In this paper, diversity coupled Vivaldi antenna elements are proposed for UWB applications [4-5]. The broadband attributes of Vivaldi antenna radiators offer effective solutions for wireless body area networks (WBAN) for achieving specifications in terms of path gain and guaranteed minimum data rates as defined in the IEEE 802.15.6-2012 standard for WBANs with low power consumption and resilience to multipath fading. The organization of the paper is built around three sections. The first section deals with the design and modelling analysis of UWB coupled Vivaldi antenna elements printed on laminate substrate. In the second section correlation analysis between full-wave time-domain and frequency-domain simulations are compared to broadband measurement.

The third section is dedicated for investigate the impact of antenna feeding lines and SMA connectors for assessing their effects on gain and radiation efficiency performances. Co-design of coupled Vivaldi antenna elements with power generation circuits for millimetre-wave communication and energy harvesting it would be like application perspectives. Energy harvesting [6-7] for the powering of wireless sensor nodes (WSN) appears as a strong technology enabler towards autonomous nomad objects.

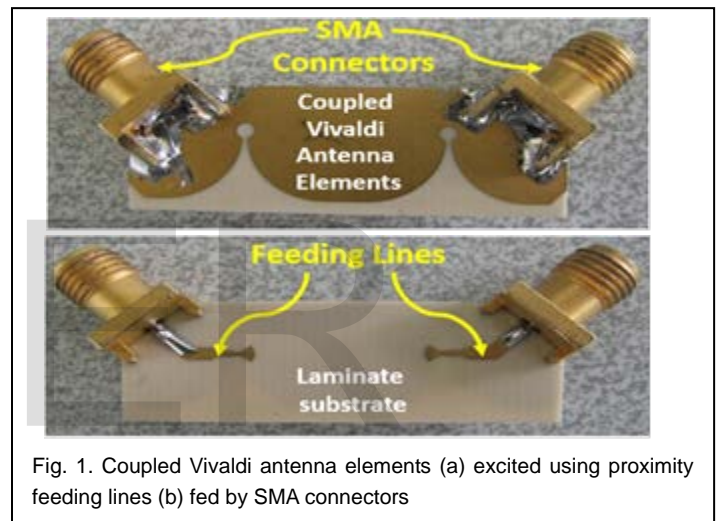


Fig. 1. Coupled Vivaldi antenna elements (a) excited using proximity feeding lines (b) fed by SMA connectors

2 BROADBAND MODELING AND EXPERIMENTAL CHARACTERIZATION OF COUPLED VIVALDI ANTENNA ELEMENTS: MAIN RESULTS AND ANALYSIS

2.1 Design, modeling and analysis

The performance of Vivaldi elements arrays such as, the broadband, directivity and gain is critically dependent on the design is achieved. We defined the design parameters of Vivaldi antenna, nature of substrate and radiating element respectively according per the following table. 1. A slight variation of parameters can influence on antenna performance [8-9].

Major advantage of this antenna type is that the UWB can be achieved using exponential tapered profiles. However, the UWB of the antenna is limited by the transition from the feed line to slot line of the antenna.

The antenna by its tapered shape plays the role of matching between the characteristic impedance of the air 120π and 50Ω . We defined the design parameters of Vivaldi antenna, nature of substrate and radiating element.

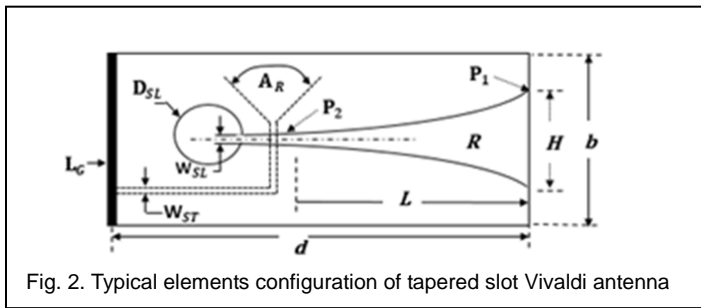


Fig. 2. Typical elements configuration of tapered slot Vivaldi antenna

- A_R : Angle of radial strip line stub.
- D_{SL} : Diameter of circular slotline cavity.
- W_{ST} : Stripline width.
- W_{SL} : Slotline width.
- L_G : Ground plane size.
- R : Opening rate.

The minimum aperture W_{SL} and the maximum aperture H are adjusted according to the highest frequency and the lowest frequency respectively of the UWB [10]. The antenna width H is determined by the lowest frequency F_{min} and effective dielectric constant (ϵ_{eff}).

$$H = \frac{c}{\sqrt{\epsilon_{eff}} \times 2 \times F_{min}} \quad (1)$$

The exponential taper profile curves employed in this structure is defined by the following function.

$$y = c_1 e^{Rz} + c_2 \quad (2)$$

C_1 and C_2 are constant, R is the opening rate defined by two point $P_1(z_1, y_1)$ and $P_2(z_2, y_2)$ and supposed as the beginning and the end [11].

$$c_1 = \frac{y_2 - y_1}{e^{Rz_2} - e^{Rz_1}}; c_2 = \frac{y_1 e^{Rz_2} - y_2 e^{Rz_1}}{e^{Rz_2} - e^{Rz_1}} \quad (3)$$

The tapered form factor used, the actual part of the in-put impedance of the antenna is of the order of 100-150 Ω . The real part of the input impedance is low when the length of antenna denoted L is long. Also, the length plays on the radiative losses.

The minimum length of the antenna to have 50 Ω makes the antenna less compact and requires shortening the antenna, but this small handicap can be compensated by the other elements of the antenna, circular slot, radial stub and auxiliary matching network on the board.

The circular slot is necessary to play the role of ending the antenna. In the first place, it behaves like a parallel inductor and compensates the capacitive effect of the antenna. More the diameter of circular slotline cavity 'DSL' is small, more the inductance is small.

The stub radial is also play the role of the termination, it allows the coupling between feed line and the antenna. Furthermore, it behaves as a serial capacity. The LC network composed by the stub radial and circular slot realize a part of impedance matching.

The auxiliary matching network is composed by the microstrip line and allows to adjust the input impedance to 50 Ω .

The designed antenna circuit is fabricated on a low-cost FR-4 substrate with 215 μm of thickness. The permittivity of substrate is taken as 3.4 with 0.01 loss tangent.

The antenna parameters are presented following table1.

TABLE 1
CHARACTERISTICS OF DUAL VIVALDI ANTENNA

Metal thickness	15 μm
Conductivity (σ : S/m)	5.96e+7
b (μm)	14287
W_{ST} (μm)	1250
W_{SL} (μm)	6750
H (μm)	11400
d (μm)	23778

The proposed structure has typical applications, ground penetrating radar (GPR), detecting hidden objects in wall and UWB communication [14].

Vivaldi antenna can be used like the first important part of energy harvesting, furthermore, the antenna can also be used like sensor for autonomous operation of small appliances.

The following section is dedicated to validate the integration of the dual Vivaldi antenna in different environments. Antenna performances have been measured in different environments such as air, solid (coffee, sugar, flour, rice) and liquid (tap water, salted water, mineral water) [16-17].

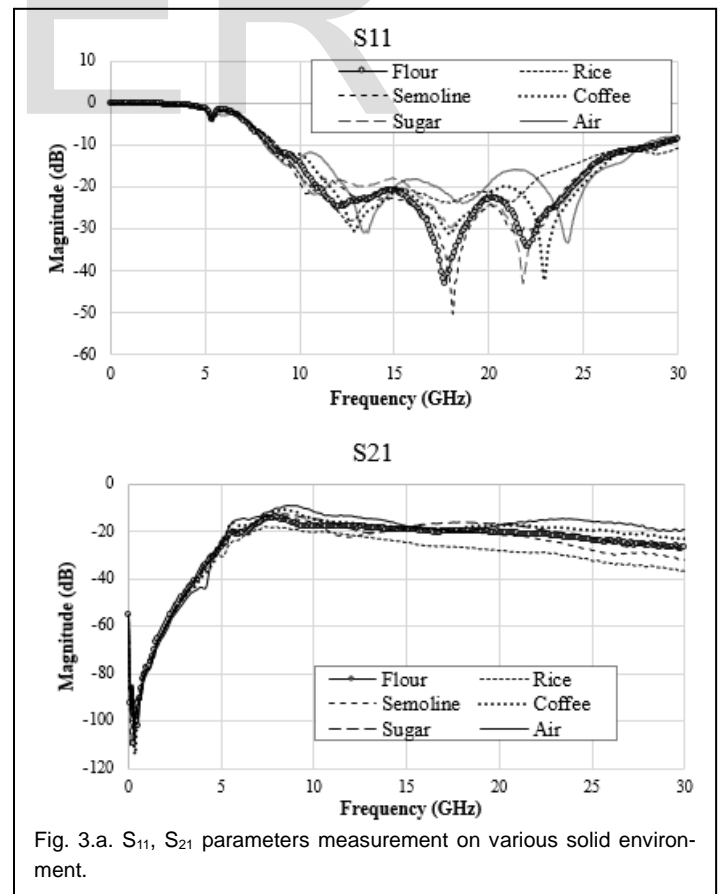


Fig. 3.a. S_{11} , S_{21} parameters measurement on various solid environment.

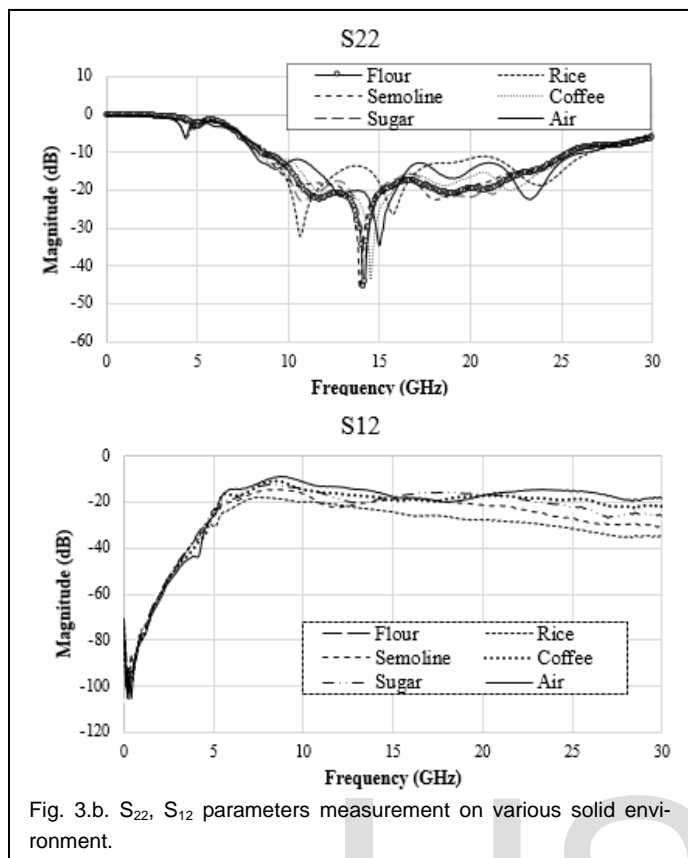


Fig. 3. b. S_{22} , S_{12} parameters measurement on various solid environment.

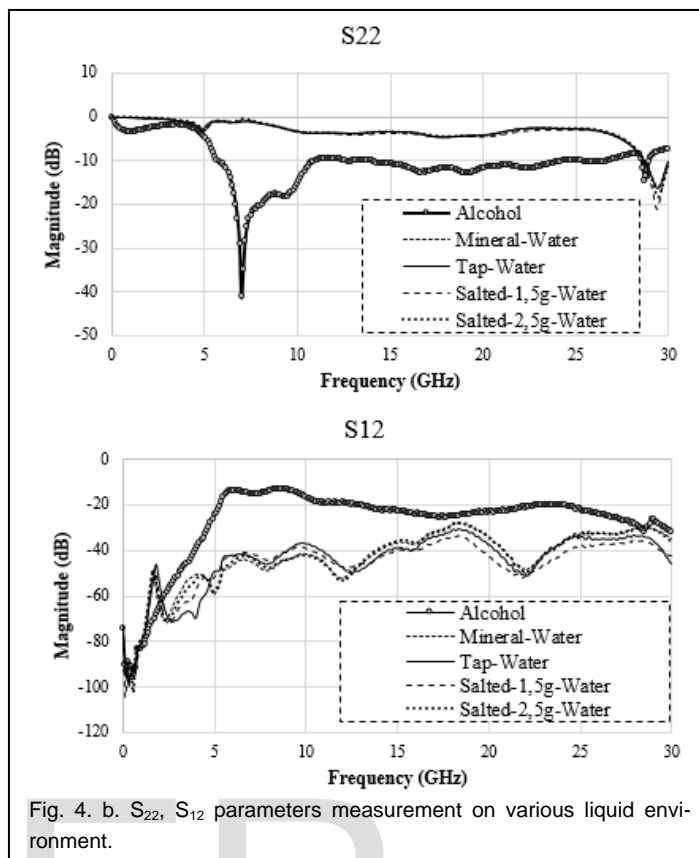


Fig. 4. b. S_{22} , S_{12} parameters measurement on various liquid environment.

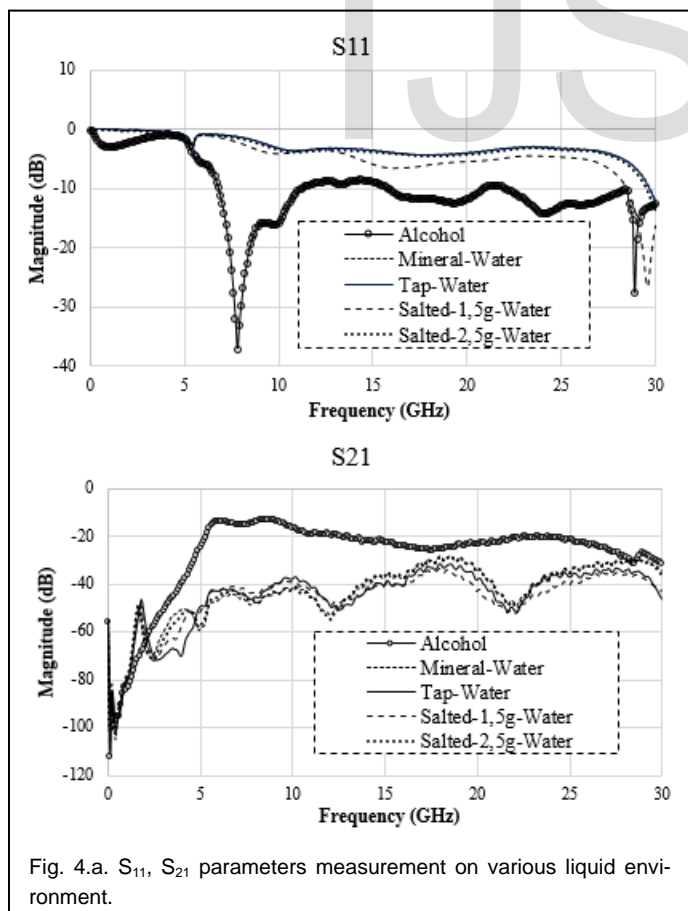


Fig. 4. a. S_{11} , S_{21} parameters measurement on various liquid environment.

The capacitive effect of the medium shifts the resonance frequencies. However, Figure. 3, illustrates the results obtained for different values of dielectric constant, varying from 1 to 4.5, the -10dB impedance bandwidth cover the bandwidth from 9.4 to 28GHz and the antenna still cover the UWB applications. The bandwidth is reduced to 5GHz on a pure alcohol medium. For high values of dielectric constant of liquid environment (epsilon 78.4), we observe an absorption of signal and this will influence the radiation and the matching performance. The syntheses of results are summarized in table 2.

TABLE 2
BANDWIDTH FOR DIFFERENT DIELECTRIC CONSTANT

Environment	Dielectric constant	Bandwidth (GHz)
Solid	1 - 4.5	[9: 28]
Liquid	68	[6:11]
	78.5 - 80.5	Absorption

The proposed antenna provides UWB coverage in different environments which allows an easy use in varied applications.

2.1 Correlation between modeling and measurement

In this section, we study the correlation analysis between full-wave time-domain and frequency-domain simulations compared to broadband measurements.

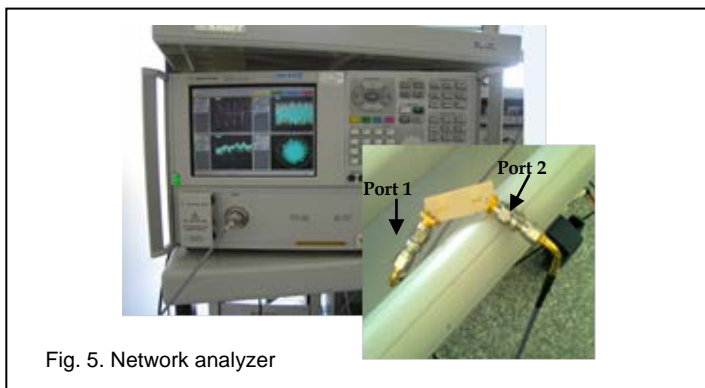


Fig. 5. Network analyzer

Before starting the measurement, the calibration is necessary to eliminate the sources of errors, a Short, Open, Load and Thru (SOLT-2port-3.5mm) has been used to compensate sources of errors.

The measured results were obtained using the Agilent vector network analyzer 50GHz. The antenna has been measured several times to approve the results obtained.

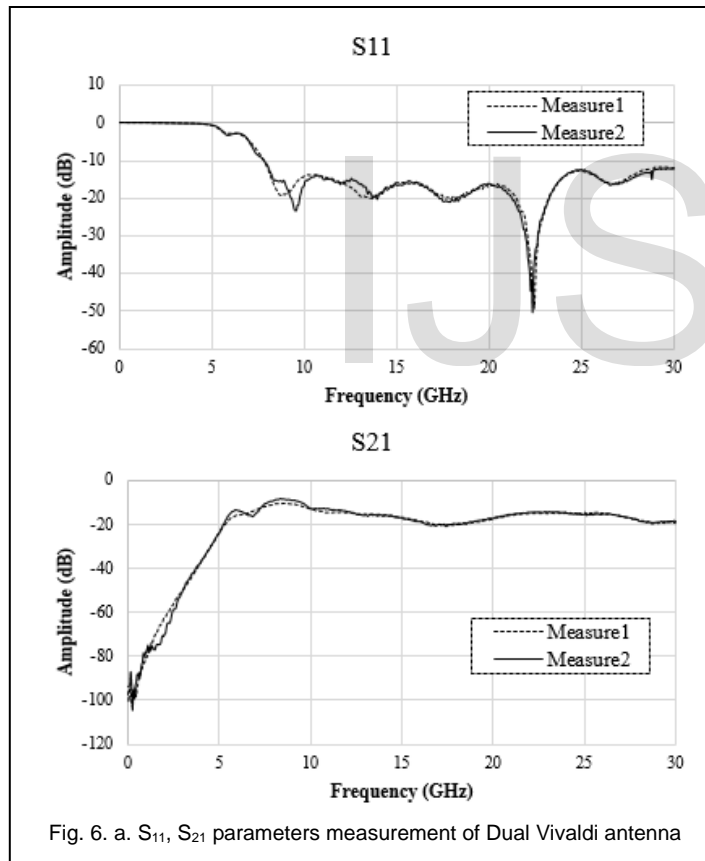


Fig. 6. a. S_{11} , S_{21} parameters measurement of Dual Vivaldi antenna

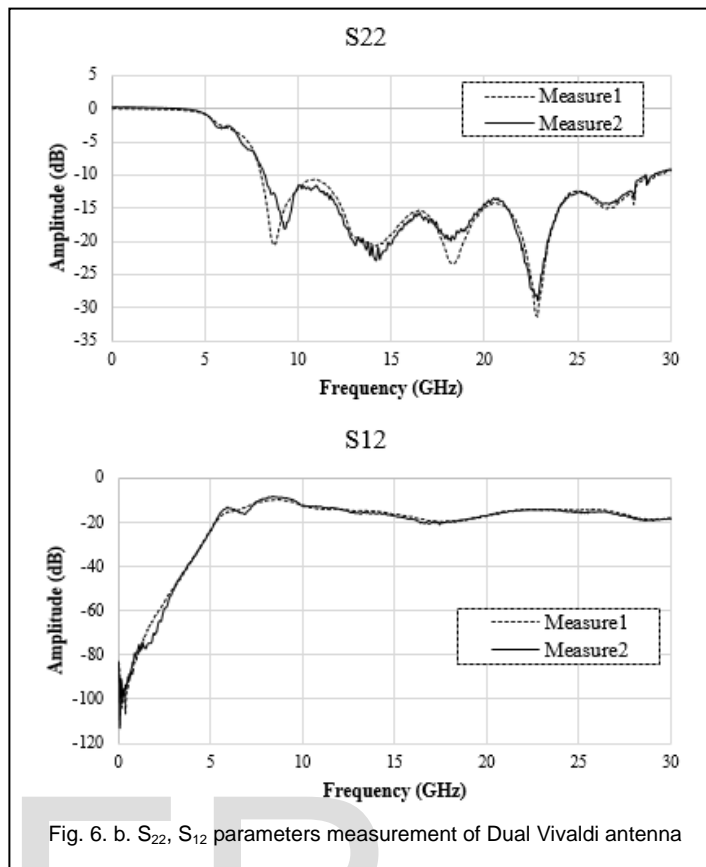


Fig. 6. b. S_{22} , S_{12} parameters measurement of Dual Vivaldi antenna

The antenna is supposed identical on both sides. However, a difference on amplitude is observed between the measurement of S_{11} on port 1 and S_{22} on port 2, could be attributed to the fabrication tolerances and the welding effects.

The proposed antenna has been analysed using a full-wave temporal domain based on finite difference time domain - FDTD-, and frequency domain based on finite element method -FEM - and method of moment -MoM- to solve Maxwell's curl equations and to predict the behaviour of the system. Simulation conditions were respected to ensure convergence, stability of the algorithm and avoid an exorbitant use of memory to obtain correct results. Absorbent boundary conditions have been applied to avoid boundary reflections, as well as the increment of step time and step grid of space for stability of the program. Non-uniform mesh has been implemented to reduce the time of calculation and increase the precision for FDTD method [14-17-18].

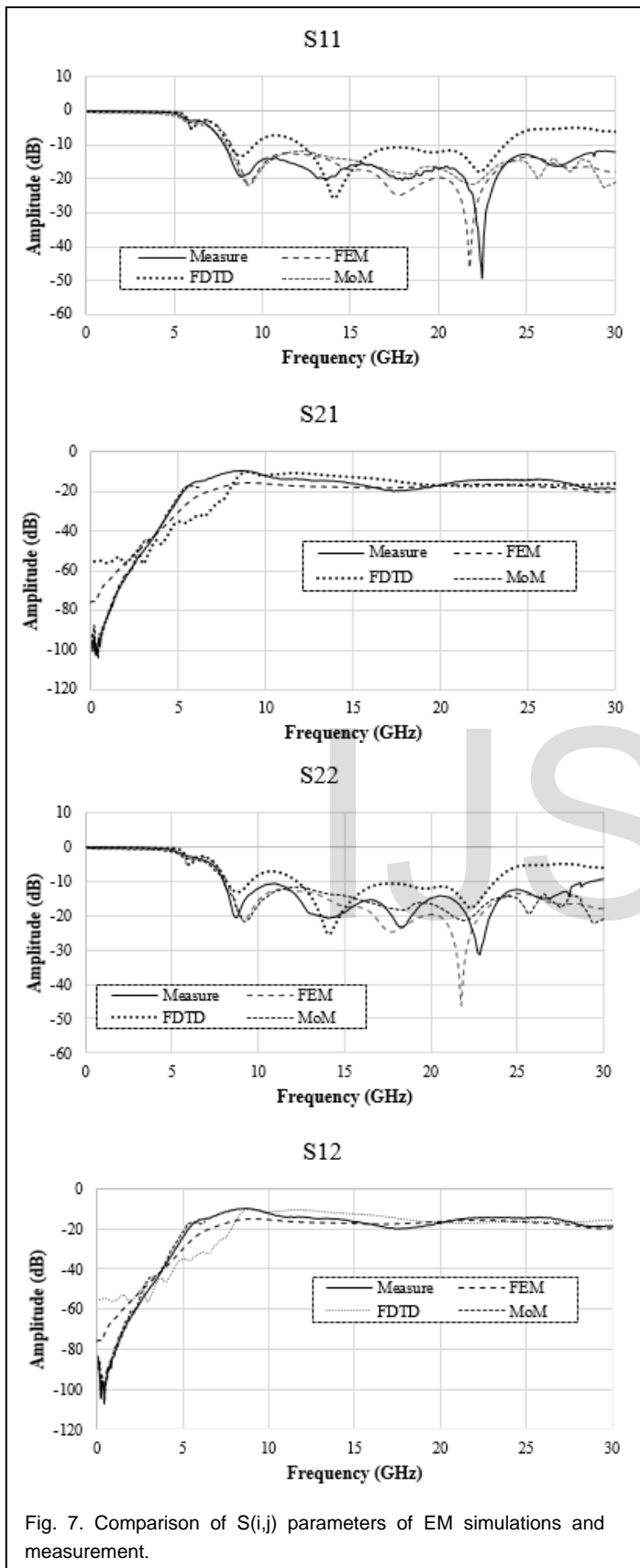


Fig. 7. Comparison of $S(i,j)$ parameters of EM simulations and measurement.

impedance bandwidth for both results cover a bandwidth 9GHz-28GHz. As can be seen from the measure plots, the amplitude attains a value of -19, -20dB, -21dB and -45dB for 9.2GHz, 13.7GHz, 18.1GHz and 22.4 GHz respectively, which makes the proposed antenna suitable to operate at this frequency, however, the proposed antenna ensures a good transmission over the UWB.

There is slight deviation between the measured and the simulated results which could be attributed to the fabrication tolerances and losses in the circuit. Also, the difference observed between the numerical methods they come from the numerical dispersion and the numerical loss. Furthermore, the FDTD method use the uniform cubic grid in the critical areas fig.1 (e.g. exponential curve, and stub angle) which explain the difference of amplitude observed on simulation [19].

The electromagnetics simulations show a good correlation with the measurement results. The comparison of both results is summarized in table 3.

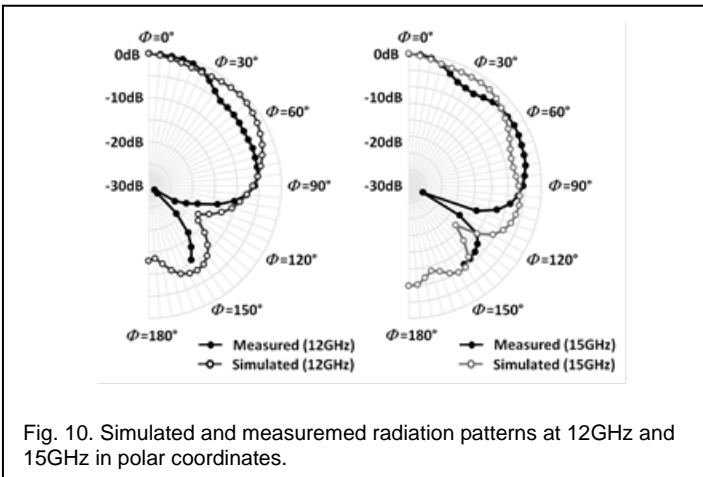
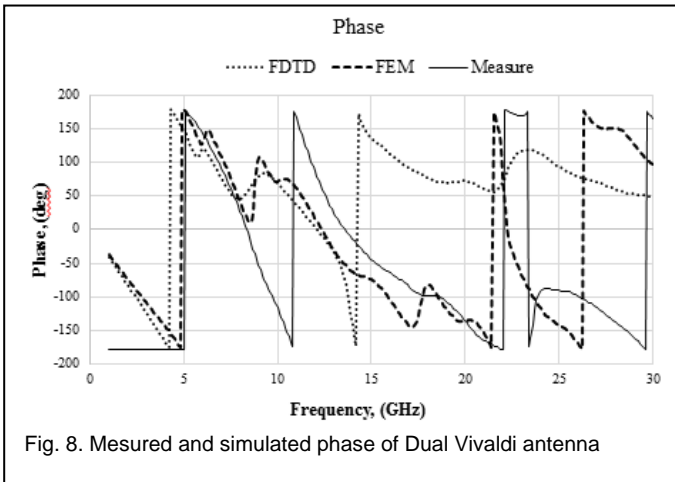
TABLE 3
ANALYSIS BETWEEN MODELING AND MEASUREMENT RESULTS

	Measure	FEM	FDTD	MOM
f_1 (GHz)	9.20	9,30	8.91	9,17
f_2 (GHz)	13.5	---	14	14.15
f_3 (GHz)	17.9	17.77	---	18.42
f_4 (GHz)	22.45	21,80	22.43	22,11
$\Delta\epsilon_1$		0.1%	3%	0.3%
$\Delta\epsilon_2$		---	3.7%	6%
$\Delta\epsilon_3$	/	1%	---	3%
$\Delta\epsilon_4$		2%	0.1%	1.5%

Furthermore, the width of each resonator is considered small compared to the width of a single resonator. This may explain why these obtained resonant frequencies didn't appear obvious in these results.

The gaps between the simulated and measured results are weak, maximum error is 6%. Indeed, during the realization of circuits, discontinuities caused by the welds defects in-creses the radiation losses. More, SMA connectors presents a source of degradation in measure. However, on modeling, the commercial software propose an ideal access ports.

Figure. 7, shows the simulated and measured return loss and transmission response of the proposed antenna. The -10dB



The phase of parameter S_{11} allows the use of antenna arrays to work together as a single antenna. By appropriately selecting the spacing between the elements and the phase of the current flowing in each of the antennas, the directivity and gain of the antenna can be modified by constructive interference in certain directions, also, to enhance the power radiated and cancelling by interfering destructively to reduce the power radiated in other directions.

3 VIVALDI ANTENNA RADIATION PERFORMANCE

3.1. Radiation pattern

Figure. 9 shows the radiated pattern performance of the proposed antenna in the directions (ϕ , θ) at the frequencies: 12.1GHz for ($\phi=90^\circ$, $\theta=120^\circ$), 15GHz for ($\phi=90^\circ$, $\theta=120^\circ$), 12GHz for ($\phi=110^\circ$, $\theta=85^\circ$) and 22GHz for ($\phi=110^\circ$, $\theta=85^\circ$).

Fig. 10. Simulated and measured radiation patterns at 12GHz and 15GHz in polar coordinates.

The simulated and measured results show good agreement despite of small discrepancies due the fixation of the Vivaldi antenna on the measuring bench, also, the undesirable fac-tors such as SMA connector, welding and fabrication error, which impacts the radiation pattern of the antenna under test.

3.2. Gain

First, the antenna was excited from a single port, then, by both ports. Figure11, shows that the dual Vivaldi antenna provides a gain greater than a single antenna. The gain is obtained in the maximum direction of radiation.

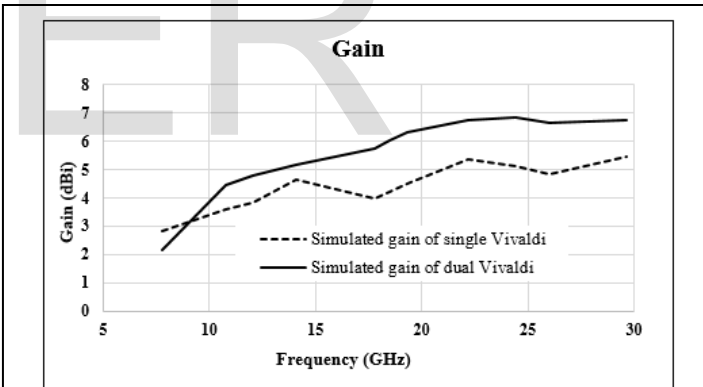
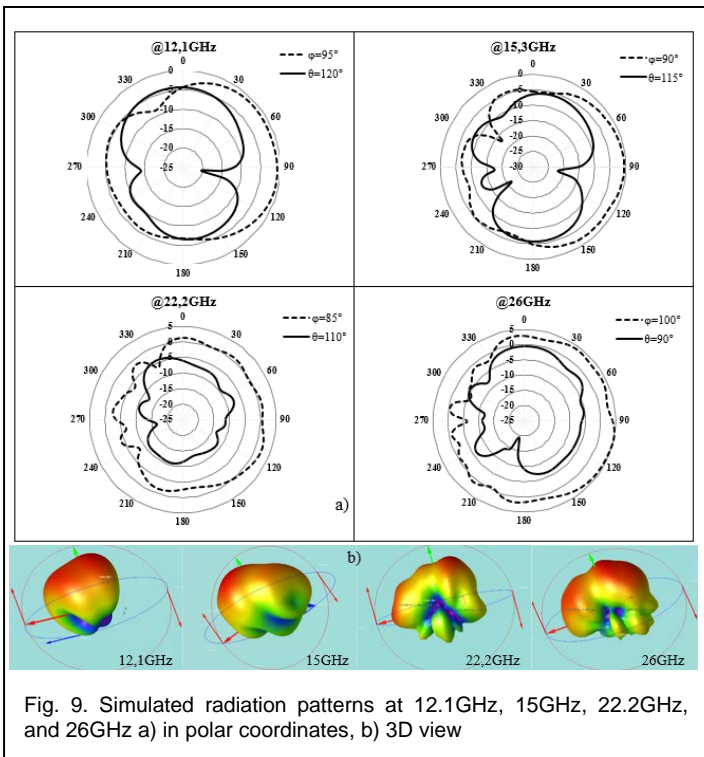


Fig. 9. Simulated radiation patterns at 12.1GHz, 15GHz, 22.2GHz, and 26GHz a) in polar coordinates, b) 3D view

Fig. 11. Simulated gain of dual Vivaldi antenna.

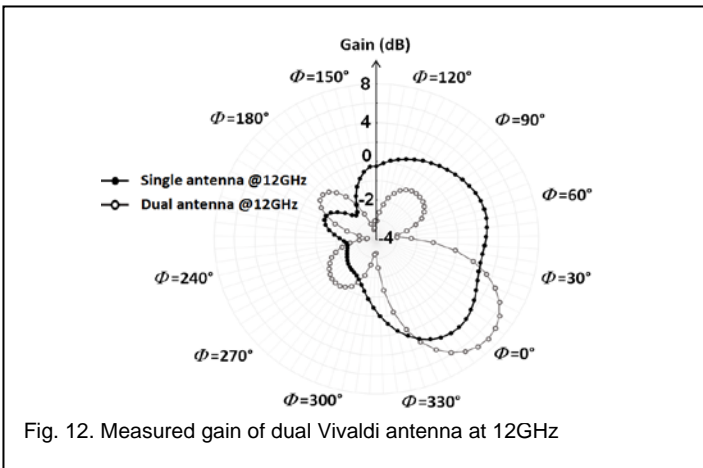


Fig. 12. Measured gain of dual Vivaldi antenna at 12GHz

The measured gain is obtained by using an absorbing material surrounding the antenna to attenuate the electromagnetic waves, then the antenna is turned over 360° to capture the intensity, figure 12, shows the measured gain of single and dual antenna at 12GHz. The proposed antenna offers high gain over 7dBi.

4 CONCLUSION

In this paper, design and modeling of a coupled Vivaldi antenna printed on a laminated substrate, operating in a UWB from 9.4GHz to 28GHz, were proposed.

The electromagnetic simulations analysis was carried out in both full wave time domain and frequency domain. Simulated results show a good correlation with measurements and confirmed the analytical calculations. Furthermore, it has been demonstrated that the antenna can operate in different media.

The proposed antenna could be integrated in several UWB applications. For future study, a co-integration of the antenna with power generation circuits for millimetre-wave communication and energy harvesting.

REFERENCES

- [1] Dardari, D., R. D'Errico, C. Roblin, A. Sibille, and M. Z. Win, "Ultrawide bandwidth RFID: The next generation?" Proc. IEEE, Vol. 98, No. 9, 1570-1582, Sep. 2010.
- [2] D. Ha and P. Schaumont, B. "Replacing cryptography with ultra wideband (UWB) modulation in secure RFID", in Proc. IEEE Int. Conf. RFID, Grapevine, TX, Mar. 2007, pp. 23-29.
- [3] Y. Shen and M. Z. Win. (2010). "Fundamental limits of wideband localization -Part I: A general framework". IEEE Trans. Inf. Theory. [Online]. 56. Available: <http://arxiv.org/abs/1006.0888>;
- [4] P.J. Gibson. "The Vivaldi aerial." Proceedings of the 9th European Microwave Conference, pages 101-105, 1979.
- [5] Ammann, M. J., McEvoy, P., Gaetano, D., Keating, L. and Horgan, F.: 'An Antenna for Footwear', MobiHealth 3rd International Conference on Wireless Mobile Communication and Healthcare, Paris, 2012, pp. 1-6.
- [6] S. Pellerano, J. Alvarado, and Y. Palaskas, "A mm-wave power harvesting RFID tag in 90 nm CMOS," in Custom Integr. Circuits Conf., San Jose, CA, Sep. 2009, pp. 677-680.
- [7] R. J. M. Vullers, R. van Schaijk, H. J. Visser, J. Penders, and C. Van Hoof, "Energy harvesting for autonomous wireless sensor networks," IEEE Solid-State Circuits Mag., vol. 2, no. 2, pp. 29-38, Spring, 2010.
- [8] S. Wang, X. D. Chen and C. G. Parini. "Analysis of ultra wideband antipodal vivaldi antennas based on inhomogeneous anisotropic zero-index metamaterials". Progress In Electromagnetics Research, Vol. 120, 235-247, 2011.
- [9] E. Gazit, "Improved design of the Vivaldi antenna," IEE Proceedings, Vol.135, pp. 89-92, April 1988.
- [10] J.P. Weem et al, "Vivaldi antenna arrays for SKA," Antennas and Propagation Society International Symposium, Vol.1, July 2000, pp. 174-177.
- [11] B. Zhou, H. Li, X. Y. Zou, and T. J. Cui, "broadband and high-gain planar vivaldi antennas based on inhomogeneous anisotropic zero-index metamaterials". Progress In Electromagnetics Research, Vol. 120, 235-247, 2011.
- [12] Ramesh Garg, Inder Bahl, Maurizio Bozzi, Book: "Microstrip Lines and Slotlines", Third Edition
- [13] V. H. Rumsey, "recency independent antennas," in, 1957, app. 114-118.
- [14] A. Godard, L. Desrumaux, V. Bertrand et al., "A transient UWB antenna array used with complex impedance surfaces," International Journal of Antennas and Propagation, vol. 2010, Article ID 243145, 8 pages, 2010. View at Publisher · View at Google Scholar · View at Scopus.
- [15] Y. Yue, D. Yunyang, J. Zhou, "An Ultra-Wideband Vivaldi Antenna Array in L and S bands" 2016 IEEE 5th Asia-Pacific Conference on Antennas and Propagation.
- [16] L. Leyssenne, S. Wane, S. Massenet, D. Bajon, C. Coq-Germanicus, P. Descamps, G. Audoit, "Electromagnetic modeling and experimental characterization of dielectric material and liquid properties from RF to THz" International conference on Electromagnetics in Advanced Applications, Pp, 1032/1035, 2013.
- [17] S. Massenet; D. Bajon; S. Wane; L. Leyssenne; R. Coq-Germanicus; P. Descamps, "Broadband characterization of dielectric materials from RF, millimeter-wave to THz frequencies accounting for anisotropy", IEEE MTT-S International Microwave Symposium (IMS2014), pp ¼, 2014.
- [18] K.S. Yee, "Numerical solution of initial boundary value problems involving Maxwell's equations in isotropic media" IEEE Trans. Antennas Propagat. Vol. AP-14, pp 302/307, May (1966).
- [19] Berenger Jean-pierre. A perfectly matched layer for the absorption of electromagnetic waves. Journal of computational physics 114, 185-200, 1994
- [20] Taflov and Allen. Book "Computational electrodynamics. finite difference temporal domain technique. Edition 1995.